

Ultrasmall Mode Volumes in Dielectric Optical Microcavities

Jacob T. Robinson, Christina Manolatu, Long Chen, and Michal Lipson

Department of Electrical and Computer Engineering, Cornell University, Ithaca, New York 14853, USA

(Received 3 May 2005; published 27 September 2005)

We theoretically demonstrate a mechanism for reduction of mode volume in high index contrast optical microcavities to below a cubic half wavelength. We show that by using dielectric discontinuities with subwavelength dimensions as a means of local field enhancement, the effective mode volume (V_{eff}) becomes wavelength independent. Cavities with V_{eff} on the order of $10^{-2}(\lambda/2n)^{-3}$ can be achieved using such discontinuities, with a corresponding increase in the Purcell factor of nearly 2 orders of magnitude relative to previously demonstrated high index photonic crystal cavities.

DOI: [10.1103/PhysRevLett.95.143901](https://doi.org/10.1103/PhysRevLett.95.143901)

PACS numbers: 42.70.Qs, 32.80.-t, 42.50.Pq, 42.82.-m

Most photonic dielectric cavities have been traditionally limited to sizes that are on the order of the wavelength of light. Cavities based on photonic crystals have been demonstrated with mode volumes as small as a few half wavelengths in each dimension [1–3]. This lower bound on the effective mode volume (V_{eff}) arises from a mechanism of confinement based on interference effects and is therefore wavelength dependent. Here, using dielectric discontinuities, we show a wavelength-independent decrease in mode volume by several orders of magnitude over previous high index dielectric microcavities.

Reducing V_{eff} in cavities enables one to control the degree of light-matter interaction for processes such as spontaneous emission, nonlinear optical responses, and strong coupling. The control of these interactions is crucial for applications in light emitting devices, as well as for optical switches and modulators [3–7]. Here we focus on the interaction of light with an emitter and analyze the enhancement of the spontaneous emission rate due to the decrease in V_{eff} . The Purcell factor (a measure of the spontaneous emission rate enhancement) for an emitter in a resonant cavity is derived directly from Fermi's golden rule [5,6]:

$$\Gamma = \frac{2\pi}{\hbar^2} \int_{-\infty}^{\infty} \langle |\vec{p}_a \cdot \alpha \vec{E}(\vec{r}_e)|^2 \rangle \rho_c(\omega) \rho_e(\omega) d\omega, \quad (1)$$

where $\rho_c(\omega)$ is the density of photon modes in the cavity, $\rho_e(\omega)$ is the mode density for the dipole transition (material emission spectrum), \vec{p}_a is the atomic dipole moment, and $\vec{E}(\vec{r}_e)$ is the electric field at the location of the emitter normalized by a factor $\alpha^2 \equiv \frac{\hbar\omega}{2} \frac{4\pi}{\int \epsilon(\vec{r}) |\vec{E}(\vec{r})|^2 d^3r}$ to the zero point energy. From Eq. (1) we see that for a given emitter with $\rho_e(\omega)$, there are two ways to increase the spontaneous emission rate. First one can increase the cavity mode density $\rho_c(\omega)$. This is commonly measured as an increase in the cavity quality factor ($Q = \omega_0/\Delta\omega$) where ω_0 is the resonant frequency and $\Delta\omega$ is resonant linewidth. Second one can increase the value of the normalized electric field at the emitter ($\alpha \vec{E}(\vec{r}_e)$). As we will show below, this amounts to decreasing the effective volume of the electro-

magnetic energy in the resonant mode (V_{eff}). Thus the common figure of merit for resonant cavities is the ratio Q/V_{eff} [4,5,8]. This can be seen from the Purcell factor (F_p) in Eq. (2). From Eq. (1) when the emitter is paced at the peak of the electric field and the cavity resonant frequency equals the peak emission frequency (ω_e), the ratio of spontaneous emission rate in the cavity compared to bulk can be written as [1,5,9]

$$\begin{aligned} F_p &= \frac{\Gamma}{\Gamma_0} = \frac{6Q(\lambda/2n)^3}{\pi^2} \frac{\epsilon(\vec{r}_{\text{max}}) \max[|\vec{E}(\vec{r})|^2]}{\int \epsilon(\vec{r}) |\vec{E}(\vec{r})|^2 d^3r} \\ &= \frac{6Q(\lambda/2n)^3}{\pi^2 V_{\text{eff}}} = \frac{6Q}{\pi^2 \tilde{V}_{\text{eff}}}, \end{aligned} \quad (2)$$

where n is the index of refraction at the peak field (\vec{r}_{max}). We define the normalized unitless effective mode volume as:

$$\begin{aligned} \tilde{V}_{\text{eff}} &= V_{\text{eff}} \left(\frac{2n(\vec{r}_{\text{max}})}{\lambda} \right)^3 \\ &= \frac{\int \epsilon(\vec{r}) |\vec{E}(\vec{r})|^2 d^3r}{\epsilon(\vec{r}_{\text{max}}) \max[|\vec{E}(\vec{r})|^2]} \left(\frac{2n(\vec{r}_{\text{max}})}{\lambda} \right)^3, \end{aligned} \quad (3)$$

where \vec{r}_{max} is the location of the maximum squared field. It is important to note that Eq. (2) is valid under the condition that the cavity's resonance linewidth is greater than the emission linewidth of the active element [1,5]. When the resonance linewidth of the cavity is much smaller than that of the emitter (as is the case at room temperature for high- Q cavities in rare-earth-metal-doped materials), $\rho_c(\omega)$ in Eq. (1) is replaced by $\delta(\omega_e)$. In this regime the "material Q " ($Q_m = \omega_e/\Delta\omega_e$ where $\Delta\omega_e$ is the linewidth of the emitter) replaces the cavity Q in Eq. (2) [1]. Thus increasing the cavity Q has no effect on the spontaneous emission rate. The only means of increasing the spontaneous emission rate in this regime is to decrease \tilde{V}_{eff} . Recently donor-type photonic crystal cavities have shown reduced \tilde{V}_{eff} by localizing light in a low index defect region [$n(\vec{r}_{\text{max}}) = 1.0$] [10]. While there has been much advancement in creating resonators with high Q factors [2,11,12],

little progress has been made in creating mechanisms for decreasing \tilde{V}_{eff} . In this work we demonstrate a method for reducing \tilde{V}_{eff} by systematically increasing the maximum value of the normalized squared field ($\frac{\max[|E(\vec{r})|^2]}{\int \epsilon(\vec{r})|E(\vec{r})|^2 d^3r}$) in Eq. (3).

We achieve an increase in the normalized maximum field by using sub-wavelength-sized dielectric material discontinuities [13]. For example, consider a one-dimensional high index contrast slab [Fig. 1(a)]. Figure 1(d) shows the field distribution of the fundamental mode in this structure for an electric field polarized normal to the interface. One can introduce an infinitesimal low index slot at the location of peak intensity oriented perpendicular to the electric field polarization. Figure 1(b) shows an example of this slot introduced in a one-dimensional slab. We recall from Maxwell's equations that the normal component of the electric displacement (D) is continuous across the boundary of two dielectrics, thus $\epsilon_L E_L = \epsilon_H E_H$ where L and H denote low and high refractive index regions, respectively. Figure 1(e) shows the new eigenmode of the slab waveguide after the introduction of a narrow slot. The unitless effective mode volume in a waveguide with an infinitesimal slot is given by:

$$\tilde{V}_{\text{eff}}^* = \frac{\int \epsilon(\vec{r})|E(\vec{r})|^2 d^3\vec{r}}{\epsilon_L |\epsilon_H / \epsilon_L E_0|^2} \left(\frac{2n_L}{\lambda}\right)^3, \quad (4)$$

where E_0 is the maximum value of the field in the high index before introducing the slot. The infinitesimal slot has a negligible effect on the integral in the numerator; therefore, the ratio of unitless mode volumes, or the Purcell

factors [see Eq. (2)], before and after the introduction of a slot is approximately given by

$$\frac{F_p}{F_p^*} = \frac{\tilde{V}_{\text{eff}}^*}{\tilde{V}_{\text{eff}}} \approx \left(\frac{\epsilon_L}{\epsilon_H}\right)^{5/2}. \quad (5)$$

The above decrease in effective mode volume is wavelength independent and can represent more than an order of magnitude reduction. For example, using dielectric materials such as air ($\epsilon = 1$) and amorphous silicon in the infrared ($\epsilon = 13.9$) results in a reduction in \tilde{V}_{eff} by a factor of over 700. Because of the normalization to the bulk spontaneous emission rate in the Purcell factor, the radiative decay rate in the cavity is proportional to the Purcell factor times the bulk index. This bulk index is different for the cavity with and without the slot since the emitter is embedded in different bulk materials (n_H for the cavity without the slot and with n_L for the cavity with the slot). Thus the increase in the spontaneous emission rate at the peak field resulting from the introduction of the slot is given as:

$$\frac{\Gamma^*}{\Gamma} = \frac{\tilde{V}_{\text{eff}}(n_L)}{\tilde{V}_{\text{eff}}^*(n_H)} \approx \left(\frac{\epsilon_H}{\epsilon_L}\right)^2. \quad (6)$$

Field enhancement in the low index region of slot waveguides has recently been demonstrated experimentally in [14] showing over 30% of the power contained in the slot region. In Figs. 1(e) and 1(f) we show the field distributions in a slab waveguide with two different slot widths shown in Figs. 1(c) and 1(d). As the slot width increases the mode no longer resembles the original mode with a discontinuity, but becomes more confined to either side of the

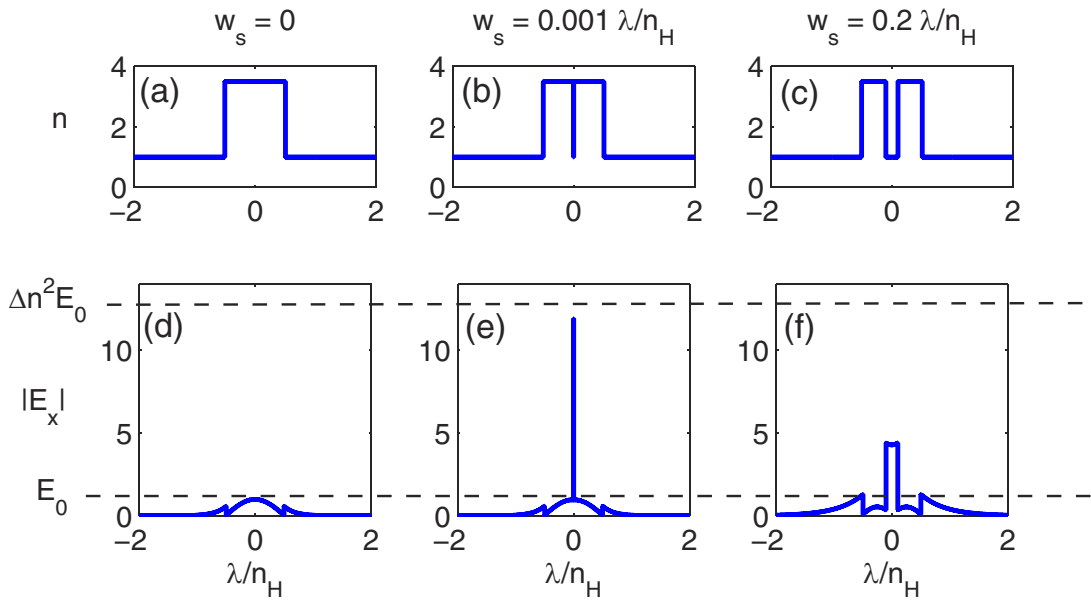


FIG. 1 (color online). (a)–(c) The index profile for the slab waveguide with embedded low index slot regions of various slot widths (w_s). (d)–(f) The field distribution of the fundamental mode in the slab waveguide for various values of w_s . The electric field is polarized normal to the interface. E_0 is the maximum value of the electric field for the slab with no slot and Δn is the ratio n_H/n_L .

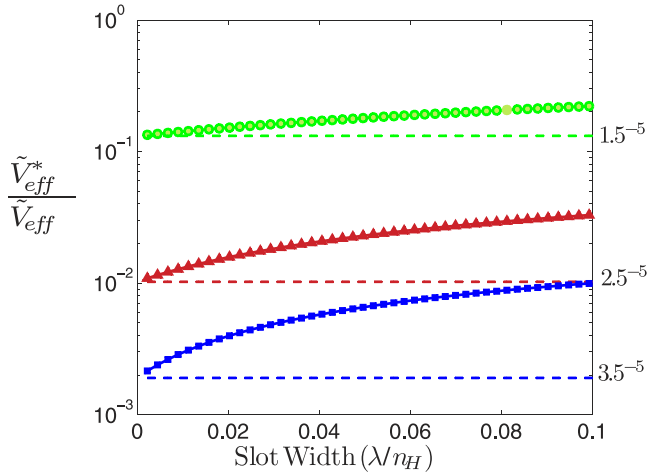


FIG. 2 (color online). The ratio of the effective mode volume of a slot waveguide compared to a slab waveguide for $\Delta n = 1.5$ (circles), $\Delta n = 2.5$ (triangles), and $\Delta n = 3.5$ (squares), where Δn is the ratio of high to low refractive indices. The slab thickness is λ/n_H .

high index material. We plot in Fig. 2 $\frac{\tilde{V}_{eff}^*}{\tilde{V}_{eff}}$ as a function of slot width for a cavity in which the field is confined in a slab waveguide of width $\lambda/2n_H$ for various index contrasts ($\Delta n = \sqrt{\epsilon_H/\epsilon_L}$). From Eq. (5) we see this ratio is equivalent to the ratio of Purcell factors in the nonslot and slot cavities. As the width of the slot narrows the relative decrease in V_{eff} approaches the dashed lines which represent the theoretical limit of Δn^{-5} given in Eq. (5).

In order to analyze the effect of the reduced mode volume on the Purcell effect, we embed the waveguide with a slot in a quasi-one-dimensional microcavity with $Q \sim 10^2$. The microcavity shown in Fig. 3(b) is a $460 \text{ nm} \times 260 \text{ nm}$ buried waveguide with refractive index of 3.48 and a cladding index of 1.46 [3]. The 1D photonic crystal on either side of the cavity consists of five 200 nm diameter holes spaced 360 nm center to center with a refractive index of 1.46. The cavity length at the center of the structure is 880 nm between the hole centers. The slot at the center of the cavity in Fig. 3(a) has a refractive index of 1.0 which is similar to recently reported fabrication [14]. Figure 3(b) shows the squared magnitude of the electric field at the resonant wavelength of 1556 nm in the cross-sectional plane at the waveguide center ($z = 130 \text{ nm}$). Figure 3(a) shows the same cavity after the introduction of a 20 nm wide slot with a refractive index of 1.0 in the cavity region. The magnitude of the electric field is determined using 3D finite difference time domain (FDTD) technique to calculate the resonant mode in each of the cavities (note that a shift of the resonance occurs, from 1556 nm to 1431 nm, when the slot is introduced due to the resulting decrease in the effective index of the cavity). Using Eq. (3) and the results of the 3D FDTD we calculate a decrease in V_{eff} from approximately

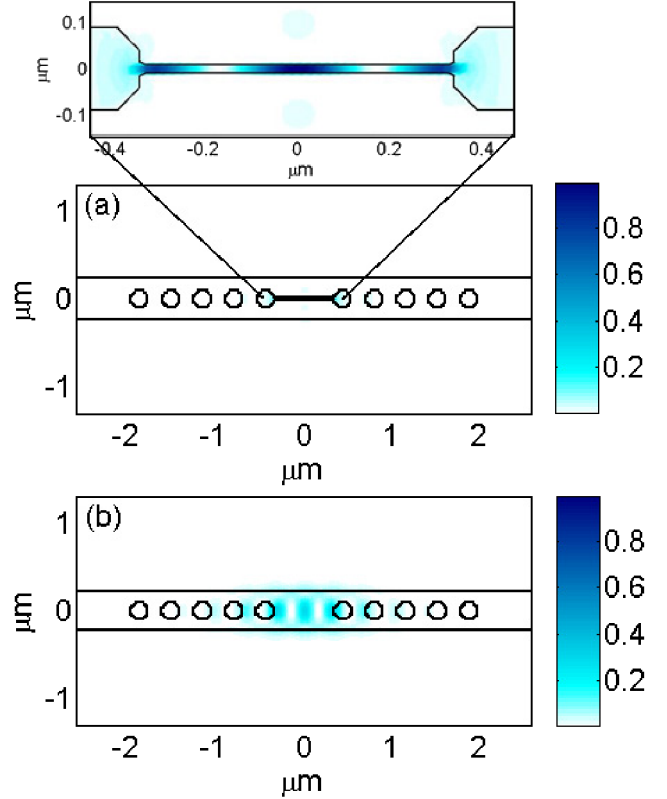


FIG. 3 (color online). (a) $|E|^2$ field spatial distribution from 3D FDTD in the a cavity based a on buried waveguide with an embedded low index slot at its resonant wavelength of 1431.3 nm. (b) $|E|^2$ field spatial distribution from 3D FDTD in a quasi-1D microcavity based on a buried waveguide without a slot for the resonant wavelength of 1556.4 nm.

$3.34(\lambda/2n)^3$ in Fig. 3(b) to $0.042(\lambda/2n)^3$ in Fig. 3(a). From Eq. (5) this corresponds to nearly an 80-fold increase in the Purcell factor and an increase in spontaneous emission rate for atoms in the cavity center by more than a factor of 20. Note from Eqs. (5) and (6) that the increase in the Purcell factor is larger than the increase in the spontaneous emission rate by a factor of n_H/n_L . The increase is smaller than the one predicted from Eqs. (5) and (6) due to the finite width of the slot. A smaller slot in the same materials could yield over 500-fold increase in the Purcell factor. The Q factor [determined by measuring the intensity decay rate of the cavity mode ($1/\tau_p$) where $Q = \omega\tau_p$ [15]] is slightly lowered by the introduction of the slot, decreasing from 305 to 175. Optimization of the cavity to better confine the new mode could be used to raise the new Q factor [16].

Note that the Purcell formalism described above in Eqs. (1) and (2) is valid in the regime in which the field does not vary significantly over the size of the emitter. To verify the proposed structure is indeed in this regime, we compare the field decay length in the slot ($1/\gamma_s$) to the size of the emitter. Taking λ to be $1.55 \mu\text{m}$, for slots ranging from 0.001 to $0.2 \lambda/2n_H$, $1/\gamma_s$ is about 3 orders of magni-

tude larger than the size of an atom or ion-based emitters. Thus these structures are well within the regime described by Eq. (1) [13]. Also note that throughout the Letter we assume that the coupling of the cavity to the emitters is in the weak coupling regime; i.e., the photon lifetime (τ_p) is much smaller than the inverse of the emitter-cavity coupling frequency. In the present work, for realistic sub-micron cavities with $Q \sim 10^3$ ($\tau_p \sim 0.8$ ps) we are well within this regime.

The principle of reduction of effective mode volume, well below the dimensions of the wavelength of light, can be applied to nearly every existing microcavity resonator to enhance not only light emission but also nonlinear effects. Examples of emitters embedded in low index media that could be used are gas-phase atoms and rare-earth-metal-doped oxides. Such a reduction can enable the demonstration of effective mode volumes on the order of $10^{-2}(\lambda/2n)^3$ or smaller and increase the Purcell factor by orders of magnitude. This technique may enable new experiments in cavity quantum electrodynamics, ultrasensitive single atom detection, and low threshold lasers.

The authors would like to thank Shanhui Fan for useful discussions. This work was supported by the Science and Technology Centers program of the National Science Foundation (NSF) under agreement DMR-0120967, the Semiconductor Research Corporation under Grant No. 2005-RJ-1296, the Cornell Center for Nanoscale Systems, the Cornell Center for Material Research, and the National Science Foundation's CAREER Grant No. 0446571. The authors would also like to thank Gernot Pomrenke from the Air Force Office of Scientific Research for supporting the work under Grants No. F49620-03-1-0424 and No. FA9550-05-C-0102.

- [1] R. Coccioli, M. Boroditsky, K. W. Kim, Y. Rahmat-Samii, and E. Yoblonovitch, *IEEE Proceedings Optoelectronics* **145**, 391 (1998).
- [2] O. Painter, K. Srinivasan, J.D. O'Brien, A. Scherer, and P.D. Dapkus, *J. Opt. A Pure Appl. Opt.* **3**, S161 (2001).
- [3] J.S. Foresi, P.R. Villeneuve, J. Ferrera, E.R. Thoen, G. Steinmeyer, S. Fan, J.D. Jannopoulos, L.C. Kimerling, H.I. Smith, and E.P. Ippen, *Nature (London)* **390**, 143 (1997).
- [4] K.J. Vahala, *Nature (London)* **424**, 839 (2003).
- [5] *Confined Electrons and Photons: New Physics and Applications*, edited by E. Burstein and C. Weisbuch (Plenum, New York, 1994).
- [6] B. Gayral, J.M. Gérard, A. Lemaître, C. Dupuis, L. Manin, and J.L. Pelouard, *Appl. Phys. Lett.* **75**, 1908 (1999).
- [7] V. Almeida, C.A. Barrios, R.R. Panepucci, and M. Lipson, *Nature (London)* **431**, 1081 (2004).
- [8] Y. Akahane, T. Asano, B.-S. Song, and S. Noda, *Nature (London)* **425**, 944 (2003).
- [9] E.M. Purcell, *Phys. Lett.* **69**, 681 (1946).
- [10] J. Vučković, M. Lončar, H. Mabuchi, and A. Scherer, *Phys. Rev. E* **65**, 016608 (2002).
- [11] Y. Akahane, T. Asano, B.-S. Song, and S. Noda, *Opt. Express* **13**, 1202 (2005).
- [12] D.K. Armani, T.J. Kippenberg, S.M. Spillane, and K.J. Vahala, *Nature (London)* **421**, 925 (2003).
- [13] V.R. Almeida, Q. Xu, C.A. Barrios, and M. Lipson, *Opt. Lett.* **29**, 1209 (2004).
- [14] Q. Xu, V.R. Almeida, R. Panepucci, and M. Lipson, *Opt. Lett.* **29**, 1626 (2004).
- [15] C. Pollock and M. Lipson, *Integrated Photonics* (Kluwer Academic, Dordrecht, 2003).
- [16] P. Lalanne, S. Mias, and J. Hugonin, *Opt. Express* **12**, 458 (2004).